

OPTICAL DEFECT MODES IN CHIRAL LIQUID CRYSTALS

V. A. Belyakov^{a}, S. V. Semenov^b*

^a*Landau Institute for Theoretical Physics, Russian Academy of Sciences
142432, Chernogolovka, Moscow Region, Russia*

^b*Russian Research Center “Kurchatov Institute”
123182, Moscow, Russia*

Received July 6, 2010

An analytic approach to the theory of optical defect modes in chiral liquid crystals (CLCs) is developed. The analytic study is facilitated by the choice of the problem parameters. Specifically, an isotropic layer (with the dielectric susceptibility equal to the average CLC dielectric susceptibility) sandwiched between two CLC layers is studied. The chosen model allows eliminating the polarization mixing and reducing the corresponding equations to the equations for light of diffracting polarization only. The dispersion equation relating the defect mode (DM) frequency to the isotropic layer thickness and an analytic expression for the field distribution in the DM structure are obtained and the corresponding dependences are plotted for some values of the DM structure parameters. Analytic expressions for the transmission and reflection coefficients of the DM structure (CLC–defect layer–CLC) are presented and analyzed for nonabsorbing, absorbing, and amplifying CLCs. The anomalously strong light absorption effect at the DM frequency is revealed. The limit case of infinitely thick CLC layers is considered in detail. It is shown that for distributed feedback lasing in a defect structure, adjusting the lasing frequency to the DM frequency results in a significant decrease in the lasing threshold. The DM dispersion equations are solved numerically for typical values of the relevant parameters. Our approach helps clarify the physics of the optical DMs in CLCs and completely agrees with the corresponding results of the previous numerical investigations.

1. INTRODUCTION

Recently, there was a very intense activity in the field of localized optical modes, in particular, defect modes (DMs) in chiral liquid crystals (CLCs), mainly due to the prospects of reaching a low lasing threshold for mirrorless distributed feedback lasing [1–4], using the DMs as narrow-band filters [5, 6], and enhancing the nonlinear optical high-harmonic generation [7] in CLCs. The DMs existing as a localized electromagnetic eigenstate with its frequency in the forbidden band gap for the structure defect were initially investigated in three-dimensional periodic dielectric structures [5]. The corresponding DMs in CLCs and, more generally, in spiral media are very similar to the DMs in one-dimensional scalar periodic structures. They reveal anomalous reflection and transmission inside the forbidden band gap [1, 2] and allow distributed feedback lasing at a low lasing threshold [3]. The qualitative difference from the case of scalar periodic media

consists in the polarization properties. The DM in a CLC is associated with a circular polarization of the electromagnetic field eigenstate whose chirality sense coincides with the one of the CLC helix. There are two main types of defects in chiral liquid crystals studied up to now. One of them is a planar layer of some substance differing from a CLC that divides a perfect cholesteric structure into two parts and is perpendicular to the helical axes of the cholesteric structure [1]. The other one is a jump of the cholesteric helix phase at some plane perpendicular to the helical axes (without insertion of any substance at the location of this plane) [2]. Recently, numerous new types of defect layers were studied [8–14], for example, a CLC layer with the pitch differing from the pitch of two layers sandwiching the defect layer [8]. It is evident that there are many versions of the dielectric properties of the defect layer, but we restrict ourself in what follows to the above two main types of defects in CLCs.

Almost all studies of DMs in chiral and scalar periodic media were performed by means of numerical analysis, with the exceptions in [15, 16], where the known

*E-mail: bel@landau.ac.ru

exact analytic expression for eigenmodes propagating along the helix axes [17,18] were used for a general study of the DM associated with a jump of the helix phase. The approach used in [15,16] seems to be very fruitful because it allows easily understanding the DM physics, and therefore deserves further implementation in the study of DMs and, in particular, in specific cases offering essential simplification of the general relations for the DMs. In general, the helical media are the unique periodic structures admitting a simple exact analytic solution of the Maxwell equations; naturally, this advantage of the helical media compared to other periodic media has to be completely exploited in solving specific boundary value problems related to the DMs. In this paper, an analytic solution of the DM associated with an insertion of an isotropic layer in a perfect cholesteric structure is presented and some limit cases simplifying the problem are considered.

2. GENERAL EQUATIONS

To consider the DM associated with an insertion of an isotropic layer in a perfect cholesteric structure, we have to solve the Maxwell equations and a boundary value problem for the electromagnetic wave propagating along the cholesteric helix for the layered structure depicted in Fig. 1.

The Maxwell equations for a wave propagating along the helix axes have the form

$$\frac{\partial^2 \mathbf{E}}{\partial z^2} = \frac{1}{c^2} \varepsilon(z) \frac{\partial^2 \mathbf{E}}{\partial t^2}, \quad (1)$$

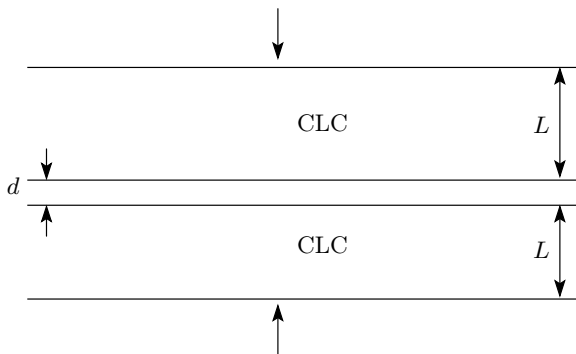


Fig. 1. Scheme of the CLC DM structure with an isotropic defect layer

where

$$\varepsilon(z) = \begin{pmatrix} \varepsilon_0 [1 + \delta \cos(\tau z)] & \pm \varepsilon_0 \delta \sin(\tau z) & 0 \\ \pm \varepsilon_0 \delta \sin(\tau z) & \varepsilon_0 [1 - \delta \cos(\tau z)] & 0 \\ 0 & 0 & \varepsilon_{\perp} \end{pmatrix} \quad (2)$$

is the dielectric tensor of the CLC [17–21] (two signs in the expression for $\varepsilon(z)$ correspond to the right and left CLC chiralities), $\varepsilon_0 = (\varepsilon_{\parallel} + \varepsilon_{\perp})/2$, $\delta = (\varepsilon_{\parallel} - \varepsilon_{\perp})/(\varepsilon_{\parallel} + \varepsilon_{\perp})$ is the dielectric anisotropy, ε_{\parallel} and ε_{\perp} are the local principal values of the liquid crystal dielectric tensor [17–22], and τ is the reciprocal lattice vector of the CLC spiral ($\tau = 4\pi/p$, where p is the cholesteric pitch).

It is well known that in a perfect cholesteric structure, i. e., in each cholesteric layer depicted in Fig. 1, there are four eigensolutions of the Maxwell equations (first studied in [17,18]), each of them being a superposition of two plane waves. Two of these eigensolutions correspond to the wave nondiffracting in the CLC and the other two correspond to the wave diffracting in the CLC and having one frequency band (around the Bragg frequency) forbidden for wave propagation (the so-called stop band). The diffracting eigensolutions are related to the circular polarization with the same sense of chirality as the chirality sense of the cholesteric helix, and the nondiffracting eigensolutions are related to the circular polarization with the opposite sense of chirality. Therefore, solving the boundary value problem requires expressing the electromagnetic wave in the CLC as a linear superposition of the four eigensolutions in each cholesteric layer of the structure depicted in Fig. 1. For the entire structure, the boundary value problem is reduced to the four problems related to the four interfaces of the structure. In addition to the parameters entering the eigensolutions (see below), the system, in particular, involves the parameter given by the ratio of the dielectric constant of the layer to the average dielectric constant of the CLC. Therefore, if we assume simple dielectric properties of the defect layer (its isotropy, for example), then the exact solution of the boundary value problem is presented analytically as a solution of the system of eight linear equations. The vanishing of the determinant of this system determines the eigensolution of the boundary value problem, i. e., the DM. However, the corresponding analytic solution and the equation for the eigenmode are sufficiently cumbersome in the general case.

An example of the exact solution of a simpler boundary value problem for a cholesteric layer sur-

rounded by an isotropic medium (the upper half in Fig. 1) is presented in [20–22].

As a result of the general analysis of solutions of the present boundary value problem and of the boundary value problem for a single cholesteric layer, we conclude that no truly localized DM exists for the boundary value problem under consideration. This is because at the isotropic layer boundaries, the diffracting eigensolutions are converted into nondiffracting eigensolutions escaping from the external cholesteric layer surfaces. In the general case, we can therefore speak of a quasilocalized DM (see also [15, 16] for the DMs related to the helix phase jump). However, in the most favorable case where the dielectric constant of the layer is equal to the average dielectric constant of the CLC, the polarization conversion is low (proportional to the dielectric anisotropy of the cholesteric). This is why in this case, for thick CLC layers, the DM is virtually completely localized (see below for the case of infinitely thick CLC layers).

In what follows, to clarify the general results, we present the explicit form of the eigensolutions and the specific cases simplifying the solution of the boundary value problem, namely, the case where the dielectric constant of the isotropic defect layer is equal to the average dielectric constant of the cholesteric and, in particular, the case of diffraction thick cholesteric layers shown in Fig. 1.

3. EIGENWAVES IN A CLC

It is known [17–21] that the eigenwaves corresponding to propagation of light along the spiral axis in a CLC, i. e., the solutions of Maxwell equation (1), are given by a superposition of two plane waves of the form

$$\mathbf{E}(z, t) = \exp(-i\omega t) \times [E^+ \mathbf{n}_+ \exp(iK^+ z) + E^- \mathbf{n}_- \exp(iK^- z)], \quad (3)$$

where ω is the light frequency, c is the speed of light, $\mathbf{n}_\pm = (\mathbf{e}_x \pm \mathbf{e}_y)\sqrt{2}$ are circular polarization vectors, where \mathbf{e}_x and \mathbf{e}_y are unit vectors along the corresponding axes, and the wave vectors K^\pm satisfy the condition

$$K^+ - K^- = \tau. \quad (4)$$

The wave vectors K^\pm in four eigensolutions of (1) are determined by Eq. (4) and the formula

$$K_j^\pm = \frac{\tau}{2} \pm \kappa \sqrt{1 + \left(\frac{\tau}{2\kappa}\right)^2 \pm \sqrt{\left(\frac{\tau}{\kappa}\right)^2 + \delta^2}}, \quad (5)$$

where $\kappa = \omega\sqrt{\varepsilon_0}/c$ and j labels the eigensolutions, with the ratio of amplitudes E^-/E^+ in (3) given by

$$\xi^j = \frac{E_j^-}{E_j^+} = \frac{\delta}{(K_j^+ - \tau)^2/\kappa^2 - 1}. \quad (6)$$

Two of the eigenwaves corresponding to the circular polarization with the chirality sense coinciding with the one of the liquid crystal spiral experience strong diffraction scattering at the frequencies in the stop band region. The other two eigenwaves, corresponding to the opposite circular polarizations, are almost unaffected by the diffraction scattering even at the stop band frequencies for the first pair.

Because the specific features of the DMs in CLCs are related to the eigenwaves of diffracting polarization (see [2, 3, 15, 16]), we restrict ourself in what follows to the consideration of the propagation of light of a diffracting polarization only.

4. BOUNDARY VALUE PROBLEM

In this section, the boundary value problem discussed above in the general form is considered under the assumption that the specific parameters allow a simplification of the problem. We assume (see Fig. 1) that the CLC is given by a planar layer with the spiral axis perpendicular to the layer surfaces. We also assume that the average CLC dielectric constant ε_0 coincides with the dielectric constant of the isotropic external medium and of the isotropic layer inserted between two cholesteric layers. This assumption allows neglecting the conversion of one circular polarization into another at the layer surfaces [20, 21] because it is proportional to the small parameter δ , the cholesteric dielectric anisotropy; the assumption also allows taking only two eigenwaves (and correspondingly only two wave vectors in Eq. (5)) with diffracting circular polarization into account.

We first consider a linear boundary value problem in the formulation where two plane waves of the diffracting polarization and of the same frequency are assumed to be incident along the spiral axis on both CLC layers (see Fig. 1) from opposite sides, and the dielectric tensor may have a nonzero imaginary part of any sign. Two diffracting eigensolutions with the structure determined by Eq. (3) are excited in both cholesteric layers. The amplitudes of the two diffracting eigenwaves are denoted by E_+^{+u} and E_-^{+u} for the upper layer and by E_+^{+d} and E_-^{+d} for the bottom layer; they have to satisfy the system of four linear equations [20, 21]

(following from the continuity of the tangential components of the electric and magnetic fields at the four boundaries of cholesteric layers depicted in Fig. 1)

$$E_+^{+u} + E_-^{+u} = E_{iu},$$

$$\begin{aligned} & \exp[i\kappa d] \exp[iK_+^+ L_-] E_+^{+u} + \\ & + \exp[i\kappa d] \exp[iK_-^+ L_-] E_-^{+u} = \\ & = \exp[iK_+^+ L_+] E_+^{+d} + \exp[iK_-^+ L_+] E_-^{+d}, \\ \xi^+ \exp[i\kappa d] \exp[iK_+^- L_-] E_+^{+u} + \xi^- \exp[iK_-^- L_-] E_-^{+u} = \\ & = \exp[i\kappa d] \xi^+ \exp[iK_+^- L_+] E_+^{+d} + \\ & + \exp[i\kappa d] \xi^- \exp[iK_-^- L_+] E_-^{+d}, \\ \exp[2iK_+^- L] \xi^+ E_+^{+d} + \exp[2iK_-^- L] \xi^- E_-^{+d} = E_{id}. \end{aligned} \quad (7)$$

Here, E_{iu} and E_{id} are the respective amplitudes of the waves of diffracting polarization incident at the cholesteric layers from the top (E_{iu}) and the bottom (E_{id}) of the structure in Fig. 1, $2L$ is the total CLC layer thickness, d is the isotropic layer thickness, $L_{\pm} = L \pm d/2$, and

$$\begin{aligned} K_{\pm}^+ &= \frac{\tau}{2} \pm q, \quad K_{\pm}^- = K_{\pm}^+ - \tau = -\frac{\tau}{2} \pm q, \\ \xi^{\pm} &= \frac{E_{\pm}^-}{E_{\pm}^+} = \frac{\delta}{(K_{\pm}^+ - \tau)^2 / \kappa^2 - 1}, \end{aligned} \quad (8)$$

where

$$q = \kappa \sqrt{1 + \left(\frac{\tau}{2\kappa}\right)^2 - \sqrt{\left(\frac{\tau}{\kappa}\right)^2 + \delta^2}}. \quad (9)$$

We note that for the further study of the DM, it is quite essential that q given by Eq. (9) is purely imaginary at the DM frequencies (located inside the stop band). The frequency at the stop band center (the Bragg frequency ω_B) is given by

$$\omega_B = \frac{2\pi c}{p\sqrt{\varepsilon_0}} = \frac{\tau c}{2\sqrt{\varepsilon_0}},$$

and the band-edge frequencies are $\omega_{\pm}^{\pm} = \omega_B / \sqrt{1 \mp \delta}$.

If we assume E_{iu} (E_{id}) to be the only nonzero amplitude, then Eqs. (7) describe the reflection and transmission of light incident on the structure (see Fig. 1) from above (below). In this case, the reflection R and transmission T coefficients of the defect structure are given by the formulas

$$R(d, L) = \xi^+ E_+^{+u} + \xi^- E_-^{+u}, \quad (10)$$

$$\begin{aligned} T(d, L) &= \exp[i(2K_+^+ L + \kappa d)] E_+^{+d} + \\ & + \exp[i(2K_-^+ L + \kappa d)] E_-^{+d}, \end{aligned} \quad (11)$$

obtained by solving Eqs. (7) under the assumption that only the wave incident from above exists ($E_{iu} \neq 0$, $E_{id} = 0$).

We now consider the solutions of system (7) in some specific situations in more detail.

5. PERFECT CHOLESTERIC LAYER

The case of a perfect cholesteric layer corresponds to two limits in Eqs. (7) and is considered here for completeness (the corresponding results can also be found in [20, 21]). One option corresponds to $d = 0$ and another to $d = 0$, but the thickness L of one of the layers in Fig. 1 is also equal to zero. The first and the second options respectively correspond to a perfect CLC layer of thicknesses $2L$ and L . Solving system (7) in these limits yields the following expressions for the amplitude reflection R and transmission T coefficients of a CLC layer of thickness L :

$$\begin{aligned} R(L) &= i\delta \sin(qL) \left\{ \frac{q\tau}{\kappa^2} \cos(qL) + \right. \\ & + i \left[\left(\frac{\tau}{2\kappa}\right)^2 + \left(\frac{q}{\kappa}\right)^2 - 1 \right] \sin(qL) \left. \right\}^{-1}, \\ T(L) &= \exp\left(\frac{i\tau L}{2}\right) \frac{q\tau}{\kappa^2} \left\{ \frac{q\tau}{\kappa^2} \cos(qL) + \right. \\ & + i \left[\left(\frac{\tau}{2\kappa}\right)^2 + \left(\frac{q}{\kappa}\right)^2 - 1 \right] \sin(qL) \left. \right\}^{-1}, \end{aligned} \quad (12)$$

where the phases of T and R correspond to the assumption that the coordinate $z = 0$ at the entrance surface and correspondingly the director orientation at the entrance surface are determined by expression (2) for the dielectric tensor $\varepsilon(z)$ of the cholesteric liquid crystal at $z = 0$ (see also [18–21]).

6. REFLECTION AND TRANSMISSION FOR THE DEFECT-MODE STRUCTURE

As we have noted, system (7) determines the amplitude light transmission $T(d, L)$ and reflection $R(d, L)$ coefficients for the DM structure (see (10) and (11)) if one of the amplitudes, E_{iu} or E_{id} , is assumed to vanish. For a finite value of L , we have to solve system (7) and use Eqs. (10) and (11) to find the transmission and reflection coefficients.

But there is another possibility to obtain formulas for the optical properties of the structure depicted in Fig. 1. If we use expressions (12) for the amplitude transmission and reflection coefficients for a single cholesteric layer (see also [20, 21]), then the corre-

sponding intensity coefficients $|T(d, L)|^2$ and $|R(d, L)|^2$ for the entire structure can be represented as

$$|T(d, L)|^2 = \left| T_e T_d \frac{\exp(i\kappa d)}{1 - \exp(2i\kappa d) R_d R_u} \right|^2, \quad (13)$$

$$\begin{aligned} |R(d, L)|^2 &= \\ &= \left| R_e + R_u T_e T_u \frac{\exp(2i\kappa d)}{1 - \exp(2i\kappa d) R_d R_u} \right|^2, \end{aligned} \quad (14)$$

where $R_e(T_e)$, $R_u(T_u)$, and $R_d(T_d)$ are the respective amplitude reflection (transmission) coefficients of the CLC layer in (12) (see Fig. 1) for the light incidence on the outer top layer surface, for the light incidence on the inner top CLC layer surface from the inserted defect layer, and for the light incidence on the inner bottom CLC layer surface from the inserted defect layer. It is assumed in deriving Eqs. (13) and (14) that the external beam is incident on the structure from above only.

We also easily find the expressions for the eigenmode amplitudes excited by the incident wave on both CLC layers of the structure depicted in Fig. 1 by using the expressions for the amplitude transmission and reflection coefficients in Eqs. (13) and (14). The eigenmode amplitudes at the CLC entrance layer are expressed in terms of $R(d, L)$ as

$$\begin{aligned} E_+^{+u} &= E_{iu} \frac{\xi^- - R(d, L)}{\xi^- - \xi^+}, \\ E_-^{+u} &= -E_{iu} \frac{\xi^+ - R(d, L)}{\xi^- - \xi^+}. \end{aligned} \quad (15)$$

The eigenmode amplitudes at the CLC exit layer are expressed in terms of $T(d, L)$ similarly, as

$$\begin{aligned} E_+^{+d} &= E_{iu} \frac{\xi^- T(d, L)}{\xi^- - \xi^+} \exp[-i(2K_+^+ L + \kappa d)], \\ E_-^{+d} &= -E_{iu} \frac{\xi^+ T(d, L)}{\xi^- - \xi^+} \exp[-i(2K_-^+ L + \kappa d)]. \end{aligned} \quad (16)$$

The corresponding calculations of the amplitudes E_+^{+u} , E_-^{+u} , E_+^{+d} , and E_-^{+d} of the eigenwaves excited in the layer (see Sec. 7) reveal a nontrivial frequency dependence of these amplitudes. Namely, close to the DM frequencies (inside the stop band, see below), the eigenmode amplitudes change sharply. However, in contrast to the corresponding amplitude changes for localized edge modes, where the changes are huge [22], the amplitude changes are of the order of unity in the case of the DM. Nevertheless, an essential enhancement of the field magnitude relative to the incident wave amplitude (in calculations, the incident wave amplitude is

assumed to be equal to unity) close to the defect layer occurs. The reason is in an exponential increase in the field as the distance from the CLC layer external surface toward the defect layer increases. As the result, the thicker a layer is, the higher the enhancement of the field at the defect layer.

7. NONABSORBING LIQUID CRYSTAL

We consider the formulas in the preceding section in more detail for nonabsorbing cholesteric layers. The calculated reflection $|R(d, L)|^2$ and transmission $|T(d, L)|^2$ spectra at normal incidence inside the stop band for the structure in Fig. 1 are presented in Fig. 2. The maxima in $|T(d, L)|^2$ and minima in $|R(d, L)|^2$ at some frequencies inside the stop band at positions that depend on the defect layer thickness d are shown. It is known [1–3, 15, 16] that the corresponding minima of $|R(d, L)|^2$ and maxima of $|T(d, L)|^2$ correspond to the DM frequencies. For the layer thickness $d = p/4$, which is half of the dielectric tensor period in a CLC, these maxima and minima are located just at the stop band center. In the interval $0 < d/p < 0.5$, the DM frequency value moves from the high-frequency stop band edge to the low-frequency stop band edge. As the defect-layer thickness increases further, the DM frequency oscillates between the high-frequency and low-frequency stop band edges. However, this is true if only $\Delta\kappa d$ is less than approximately 2π , where $\Delta\kappa$ is the change of the wave vector at the frequency width of the stop band. When $\Delta\kappa d$ exceeds 2π , the second DM frequency appears in the stop band. As d increases further, additional DM frequencies appear, whose number may be estimated as $\Delta\kappa d/2\pi$. The described appearance of many DM frequencies inside the stop band is illustrated in Fig. 3, where only $|T(d, L)|^2$ or $|R(d, L)|^2$ is presented because $|R(d, L)|^2 + |T(d, L)|^2 = 1$ for a nonabsorbing structure.

Figure 2 shows that the reflection vanishes at some frequency. From (14), we find the equation for the frequencies of the reflection coefficient zeros:

$$R_e (1 - e^{2i\kappa d} R_d R_u) + R_u T_e T_u e^{2i\kappa d} = 0. \quad (17)$$

It is quite instructive to compare the frequency dependence of the reflection coefficient and of the eigenmode amplitudes E_+^{+u} , E_-^{+u} , E_+^{+d} , and E_-^{+d} excited in the defect structure. Comparing Figs. 2 and 3 with Fig. 4 shows that the positions of the sharp amplitude oscillations just coincide with (or are very close to, for an absorbing or amplifying liquid crystal) the positions of reflection coefficient minima corresponding

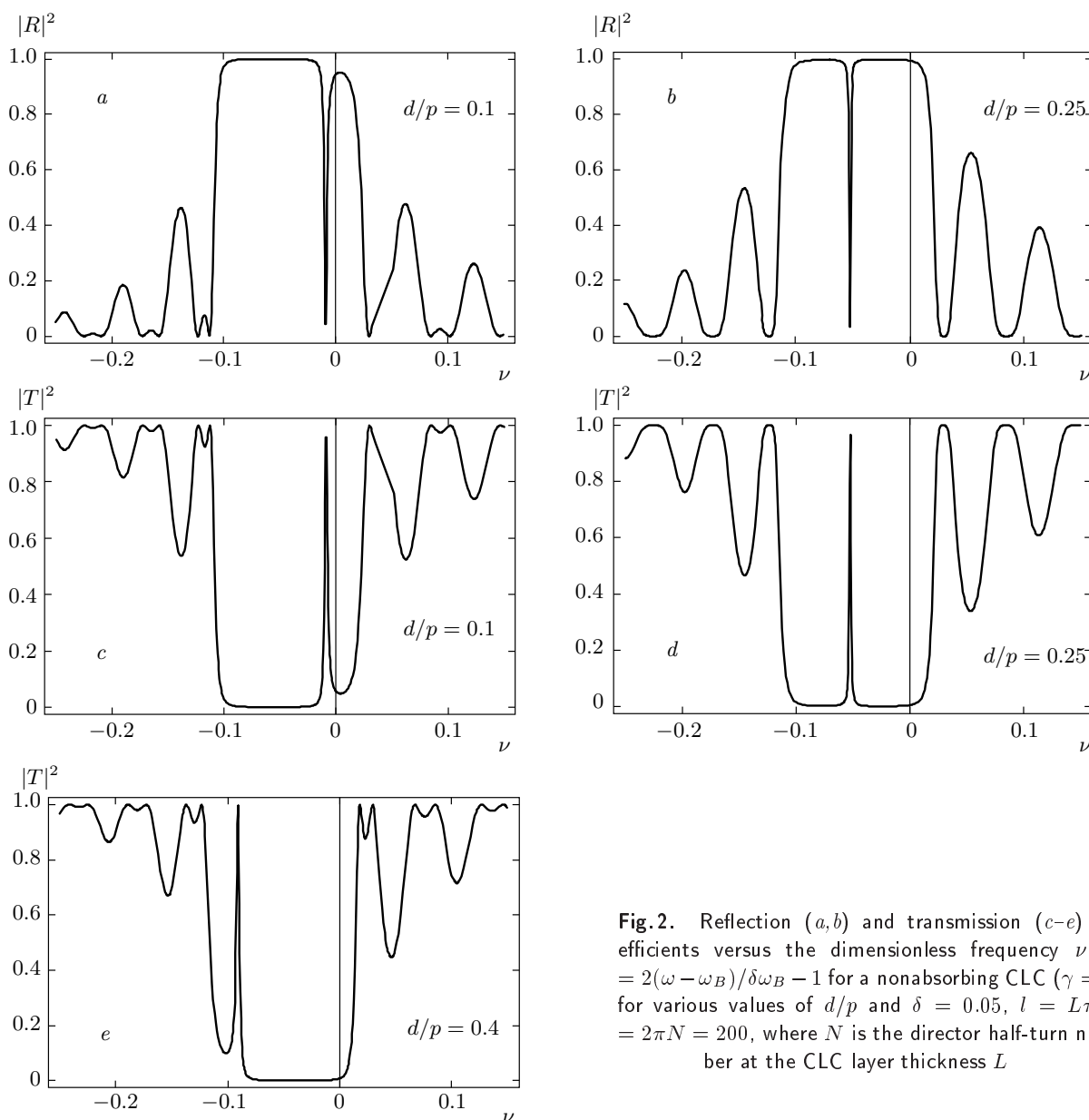


Fig.2. Reflection (*a, b*) and transmission (*c-e*) coefficients versus the dimensionless frequency $\nu = 2(\omega - \omega_B)/\delta\omega_B - 1$ for a nonabsorbing CLC ($\gamma = 0$) for various values of d/p and $\delta = 0.05$, $l = L\tau = 2\pi N = 200$, where N is the director half-turn number at the CLC layer thickness L

to $R(d, L) = 0$ for the nonabsorbing CLC. This may be considered as an indication of the existence of eigenstates of DM structures just at these frequencies.

8. DEFECT MODE (A NONABSORBING LIQUID CRYSTAL)

The solution of Eq. (7) in the general case is a linear superposition of a propagating wave and a pure DM, i. e., a standing wave of a complicated structure (not reduced to two plane counter-propagating waves). The pure DM is determined by Eq. (7) with $E_{iu} = E_{id} = 0$,

i. e., in the case where no waves are incident from outside on the structure shown in Fig. 1.

The DM frequency ω_D is determined by the zero value of the determinant of system (7):

$$\det(d, L) = 4e^{2i\kappa d} \sin^2(qL) - \frac{4e^{-i\tau L}}{\delta^2} \times \left\{ \frac{\tau q}{\kappa^2} \cos(qL) + i \left[\left(\frac{\tau}{2\kappa} \right)^2 + \left(\frac{q}{\kappa} \right)^2 - 1 \right] \times \sin(qL) \right\}^2. \quad (18)$$

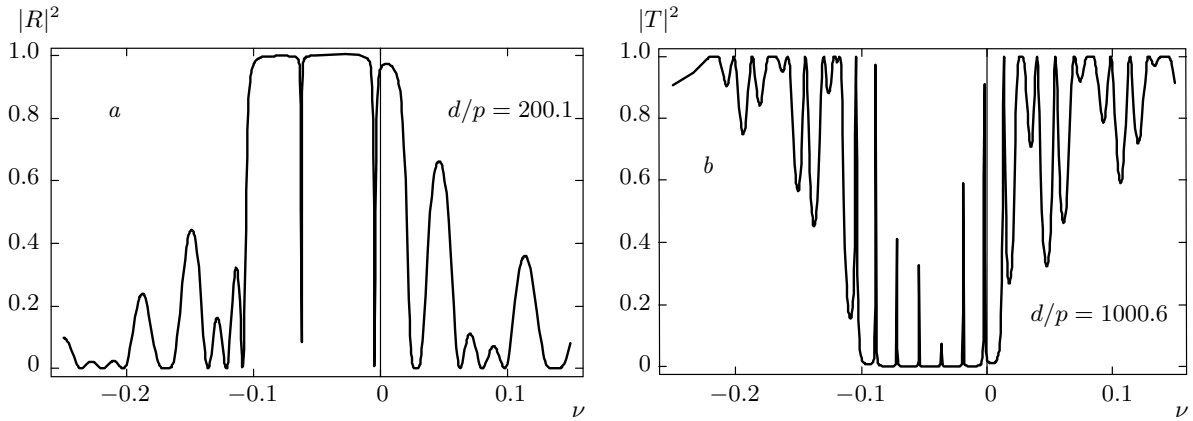


Fig. 3. Reflection (a) and transmission (b) coefficients versus the dimensionless frequency for a nonabsorbing CLC for various d/p , $\delta = 0.05$, and $N = 33$

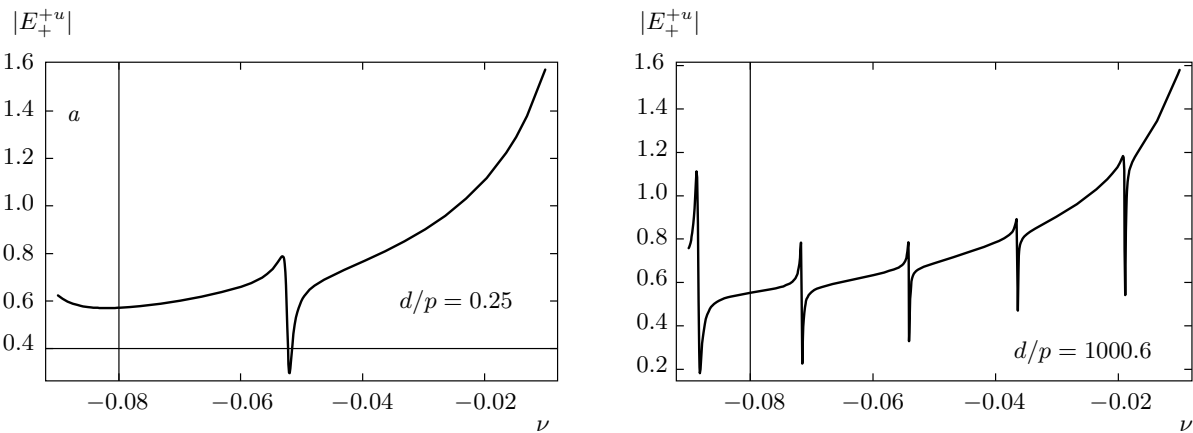


Fig. 4. The calculated eigenmode amplitude ($|E_+^{+u}|$) at the external surface of a CLC layer of the DM structure excited by the incident wave of a unit amplitude for two values of d/p , $\delta = 0.05$, and $N = 33$

We note that at a finite length L , $\det(d, L)$ does not reach zero for a real value of ω for a nonabsorbing CLC, but reaches zero for a complex value of ω . The larger the thicknesses L of the CLC layers in the DM structure (see Fig. 1) are, the smaller the imaginary part of ω is; in the limit of infinite L , it reduces to zero in the accepted approach (see Sec. 9 below). Therefore, the DM is a quasistable mode and its lifetime is determined by the imaginary part of ω_D .

Using Eqs. (13) and (14), the dispersion equation following from (18) can be reduced to the expression containing the reflection coefficients R of the CLC layers:

$$1 - R_d R_u e^{2i\kappa d} = 0. \tag{19}$$

The DM field in the CLC is a superposition of two CLC eigenmodes with their amplitudes satisfying the condition

$$E_+^{+u} + E_-^{+u} = 0. \tag{20}$$

Relation (20) allows finding the DM field inside the CLC layers using expression (3) for the CLC eigenmodes. For example, in an individual CLC layer of the DM structure (see Fig. 1), the corresponding expression for the coordinate field amplitude distribution becomes

$$\begin{aligned} \mathbf{E}(\omega_D, z, t) = & i \exp(-i\omega_D t) \times \\ & \times \left\{ \mathbf{n}_+ \exp\left(\frac{i\tau z}{2}\right) \sin(qz) + \frac{\mathbf{n}_-}{\delta} \exp\left(-\frac{i\tau z}{2}\right) \times \right. \\ & \times \left[\left(\left(\frac{\tau}{2\kappa}\right)^2 + \left(\frac{q}{\kappa}\right)^2 - 1 \right) \sin(qz) - \right. \\ & \left. \left. - i \frac{\tau q}{\kappa^2} \cos(qz) \right] \right\}, \tag{21} \end{aligned}$$

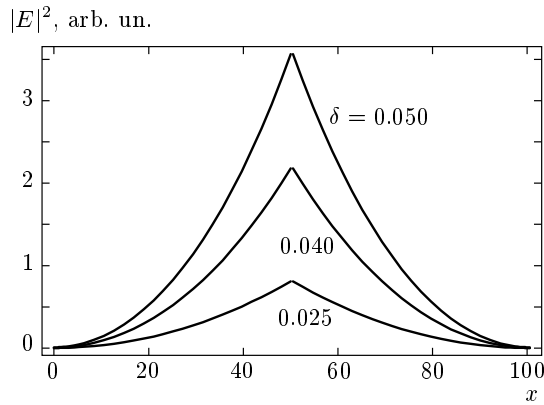


Fig. 5. Coordinate dependence ($x = z/p$) of the squared DM field at the DM frequency being at the stop band center for various dielectric anisotropy δ values and the defect layer thickness $d = p/4$ for the cholesteric layer thickness $L = 50(p/2)$

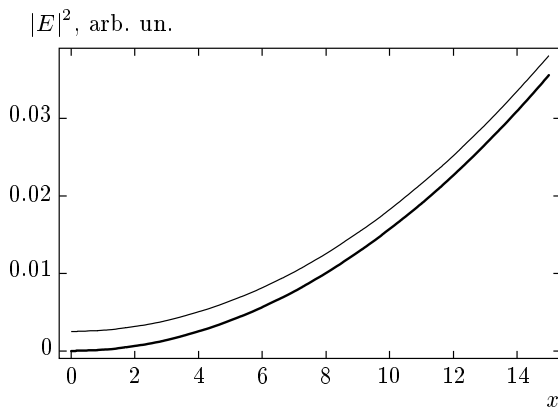


Fig. 6. Coordinate dependence ($x = z/p$) of the squared amplitude of the DM waves inside the CLC layer directed toward the defect layer (bold line) and out of the DM structure (narrow line) at the DM frequency being at the stop band center for the dielectric anisotropy $\delta = 0.05$ close to the external surface of the CLC layer

where q is determined by Eq. (9) and $z = 0$ corresponds to the external surface of the CLC layer.

The coordinate dependence of the squared modulus of the total field and its parts related to the wave propagating toward the defect layer and in the opposite direction close to the external surface of the CLC layer are presented at Figs. 5 and 6. Figure 5 shows that the larger the dielectric anisotropy δ is, the sharper the growth of the DM field toward the defect layer. Figure 6 shows that at the external surfaces of the DM structure, only the amplitude of the wave directed toward

the defect layer reduces strictly to zero. The amplitude of the wave directed outward is small, but it does not reduce to zero. This is why there is a leakage of the DM energy outward through the external surfaces of the DM structure. The ratio of the corresponding energy flow to the total DM energy accumulated in its structure determines the inverse lifetime (and correspondingly the DM frequency width), which may be presented by an analytic expression.

For nonabsorbing CLC layers (which are under the consideration in this section), the only source of decay is the energy leakage through their external surfaces. The decrease in the DM energy in unite time is equal to the energy flow of the leaking waves $(2c/\sqrt{\epsilon_0})|E_{out}|^2$, where E_{out} is the amplitude of the wave exiting the DM structure through the external surfaces of CLC layers, and therefore, using (21), we easily obtain the DM lifetime τ_D as

$$\begin{aligned} \tau_D &= \int |\mathbf{E}(\omega_D, z, t)|^2 dz \times \\ &\times \left(\frac{d}{dt} \int |\mathbf{E}(\omega_D, z, t)|^2 dz \right)^{-1} = \\ &= \frac{|E_{out}|^{-2}}{2c/\sqrt{\epsilon_0}} \int |\mathbf{E}(\omega_D, z, t)|^2 dz = \\ &= \left(\frac{\delta \kappa^2}{\tau q} \right)^2 \frac{L\sqrt{\epsilon_0}}{2c} \left\{ \left| 1 - \frac{2}{qL} \sin 2(qL) \right| \times \right. \\ &\times \left(1 + \frac{1}{\delta^2} \left[\left(\frac{\tau}{2\kappa} \right)^2 + \left(\frac{q}{\kappa} \right)^2 - 1 \right]^2 \right) + \\ &\left. + \frac{1}{\delta^2} \left| \left(\frac{\tau q}{\kappa^2} \right)^2 \left[1 + \frac{2}{qL} \sin 2(qL) \right] \right| \right\}, \quad (22) \end{aligned}$$

where the integration due to the symmetry of the DM structure is restricted to one half of the structure only. The analysis of Eq. (22) shows that the DM lifetime τ_D depends on the position of its frequency ω_D inside the stop band and reaches a maximum for ω_D just at the middle of the stop band, i. e., at $\kappa = \tau/2$.

In the general case, the description of the DM requires solving dispersion equation (18) numerically. But because $\text{Re}\omega_D$ is determined by the frequencies corresponding to the zeros of the reflection coefficient for nonabsorbing CLC layers, it is easier to investigate DMs in general. In particular, because the DM lifetime can be written as $1/\text{Im}\omega_D$, Eq. (22) for the lifetime τ_D may be used for calculating $\text{Im}\omega_D$. There are also limit cases simplifying the description of the DM considered below. As the analysis shows, the thicker CLC layers are, the larger τ_D and correspondingly less the DM frequency width. The DM lifetime in the limit of in-

finitely thick CLC layers is infinite in our model (this is directly shown in the next section).

9. INFINITELY THICK CLC LAYERS

We study system (7) in the simplest case of very thick cholesteric layers in Fig. 1. In this case, the amplitudes of the waves exponentially increasing toward the external surfaces of cholesteric layers have to vanish. Formally, we may put L to be infinitely large. In the cholesteric layers, nonzero amplitudes then correspond only to the eigenwaves propagating toward the isotropic defect layer. This means that in system (7), in the absence of waves incident at the DM structure from outside, the amplitudes E_{\pm}^{+u} and E_{\pm}^{+d} are equal to zero and the system reduces to the two linear equations

$$\begin{aligned} \exp(i\kappa d) \exp(iK_{\pm}^{+} L_{\pm}) E_{\pm}^{+u} &= \exp(iK_{\pm}^{+} L_{\pm}) E_{\pm}^{+d}, \\ \xi^{+} \exp(iK_{\pm}^{-} L_{\pm}) E_{\pm}^{+u} &= \\ &= \exp(i\kappa d) \xi^{-} \exp(iK_{\pm}^{-} L_{\pm}) E_{\pm}^{+d}. \end{aligned} \tag{23}$$

The DM frequency ω_D in this case is determined by a zero value of the determinant of system (23), which reduces to the relation

$$\begin{aligned} -\frac{2}{\delta} \exp[i(\kappa - q) d] \left\{ \frac{\tau q}{\kappa^2} \cos((\tau/2 - \kappa) d) + \right. \\ \left. + i \left[\left(\frac{\tau}{2\kappa} \right)^2 + \left(\frac{q}{\kappa} \right)^2 - 1 \right] \sin((\tau/2 - \kappa) d) \right\} = 0. \end{aligned} \tag{24}$$

For the light frequencies inside the selective reflection band, determinant (24) vanishes if the isotropic layer thickness d is related to the light frequency as

$$\begin{aligned} \frac{d}{p} \left(1 - \frac{\kappa}{\tau/2} \right) &= \frac{1}{2\pi} \times \\ &\times \arctg \frac{2(\tau/2\kappa) \sqrt{\sqrt{4(\tau/2\kappa)^2 + \delta^2} - 1 - (\tau/2\kappa)^2}}{2(\tau/2\kappa)^2 - \sqrt{4(\tau/2\kappa)^2 + \delta^2}}. \end{aligned} \tag{25}$$

This relation means that for any frequency inside the selective reflection band, the DM exists, but the existence condition demands a specific value of the isotropic layer thickness for each chosen frequency value.

The relation of the DM frequency to the isotropic layer thickness d given by (25) for infinitely thick CLC layers is shown in Fig. 7. Again, the DM frequency just at the stop band center corresponds to the layer thickness $d/p = 1/4$. The same results follow directly from (25) if we assume that ω_D is located just in the middle of the stop band, i. e., $\tau/2\kappa = 1$; in that case, Eq. (25) results in

$$\frac{d}{p} = \frac{1}{2\pi} \arctg \frac{2}{\sqrt{\sqrt{4 + \delta^2} - 2}} \approx \frac{1}{2\pi} \arctg \frac{4}{\delta}, \tag{26}$$

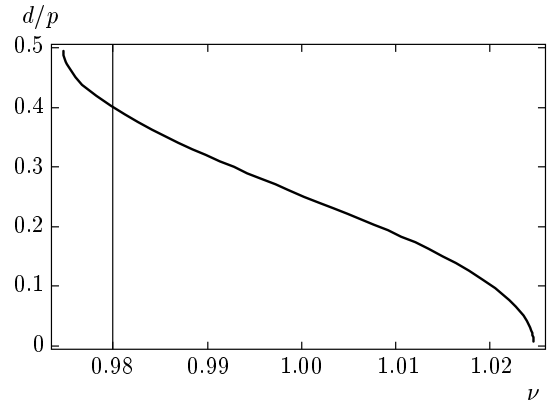


Fig. 7. Calculated relation between d/p and the DM frequency for nonabsorbing CLC layers of an infinitely large thickness ($\delta = 0.05$)

which approximately corresponds to $d/p = 1/4 + n/2$, where n is zero or an integer number.

The shift $\Delta\omega$ of the DM frequency in the interval $|\Delta\omega/\omega_B| < \delta$ due to small variations in d (Δd) close to the $d/p = 1/4$ is approximately given by the relation

$$\frac{\Delta\omega}{\omega_B} = -\frac{4\Delta d}{p}, \tag{27}$$

with the Bragg frequency (frequency at the stop band center) given below Eq. (9).

The calculations show that the DM frequency depends on the CLC layer thickness L only slightly. This is why the corresponding dependence of ω_D on d/p for an infinitely large L may be regarded as a good approximation for ω_D at any L .

It is known that the DM field is localized in the defect layer and closely by around it [1–3, 15, 16]. An illustration of such a localization is presented by the coordinate field distribution of the DM for infinitely thick CLC layers in Fig. 8. The maximum of the field amplitude is located at the defect layer and the field amplitude attenuates exponentially in the CLC outside the defect layer. The strongest attenuation occurs for the layer thickness $d/p = 1/4$, i. e., for the DM frequency just at the stop band center, with the attenuation decreasing as the DM frequency approaches the stop band edges. The attenuation also increases with an increase in the CLC layer dielectric anisotropy δ .

Equations (24)–(26) show that for infinitely thick CLC layers, the DM frequency is a real quantity in the model under consideration and hence the DM lifetime is infinite. This is not the case for a limited CLC layer thickness. For nonabsorbing CLC layers of finite thickness, determinant (18) vanishes at a complex frequency.

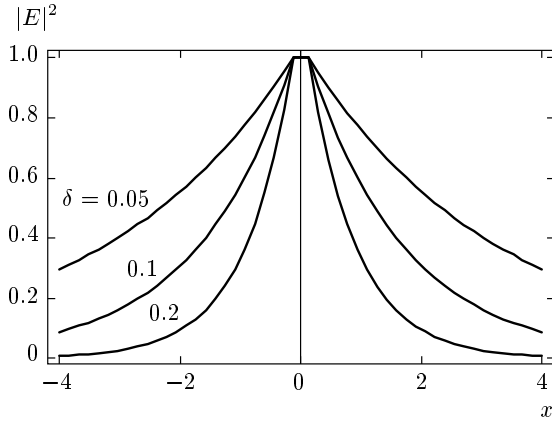


Fig. 8. Calculated distribution (see Eq. (21)) of the squared field modulus versus the distance from the defect layer center ($x = z/p$) for nonabsorbing infinitely thick CLC layers for various δ and $d/p = 1/4$

The physical meaning of the complex frequency is quite clear. As was mentioned above, for nonabsorbing CLC layers of a finite thickness, there is a leakage of the DM electromagnetic field through the external surfaces of the CLC layers, which results in a decay of the DM. Just the imaginary part of the frequency and the finite lifetime of the DM are determined by this leakage.

10. THICK CLC LAYERS

In the case of a DM structure with thick CLC layers ($|q|L \gg 1$), some analytic results related to the DM can also be obtained. These results may also be obtained from dispersion equation (18) or from expressions (13) and (14) for the DM structure transmission and reflection coefficients.

Instead of directly solving the equation for a complex frequency following from expression (18) ($\det(d, L) = 0$), we can use Eqs. (13) and (14) for the DM structure transmission and reflection coefficients to estimate the imaginary part of the DM frequency. We have to allow a nonzero imaginary addition to the frequency (defined, for example, by the relation $\omega / \text{Re}\omega = 1 + i\Delta$, where Δ is a small quantity) and search for extrema of Eqs. (13) and (14) relative to this imaginary addition $i\Delta$. The results of the corresponding calculations of the transmission $|T(d, L)|^2$ and reflection $|R(d, L)|^2$ intensity coefficients demonstrate that the imaginary addition to ω_D decreases as the CLC layer thickness increases, and the addition also decreases as $\text{Re}\omega_D$ approaches the stop band center at a fixed CLC layers thickness. In particular, the calcula-

tions show that for $d/p = 1/4$ corresponding to $\text{Re}\omega_D$ being at the stop band center, Δ is the smallest at a fixed CLC layer thicknesses. The DM lifetime τ_D determined as $\tau_D = 1 / |\text{Im}\omega_D|$ increases correspondingly as the CLC layer thickness increases, and reaches a maximum for the DM frequency at the stop band center at a fixed CLC layers thickness.

We analytically find the law of the lifetime τ increase with the CLC layer thickness, i. e., find the value of Δ (in the limit $|q|L \gg 1$) corresponding to divergence of the defect-mode structure transmission and reflection coefficients, by expanding the denominators in Eqs. (13) and (14) in the small parameter Δ .

The corresponding expression for Δ is

$$\Delta = \frac{\Delta q}{iqF(\delta^2)}, \tag{28}$$

where Δq is the change of q due to the imaginary addition to the DM frequency ω_D , ensuring the divergence of the DM structure transmission and reflection coefficients,

$$F(\delta^2) = 1 + \frac{1/2 \sqrt{(\tau/\kappa)^2 + \delta^2} - (\tau/2\kappa)^2}{1 - \sqrt{(\tau/\kappa)^2 + \delta^2} + (\tau/2\kappa)^2}$$

and

$$\Delta q = \frac{2\kappa^2}{q\tau L} \exp[-2|q|L].$$

Because the DM lifetime is $\tau_D = 1 / \text{Im}\omega_D$, expression (28) reveals an exponential increase in τ_D with an increase in the CLC thickness L , also showing a strong dependence of the increase rate on the position of ω_D inside the stop band. For the position of ω_D just in the middle of the stop band, expression (28) for Δ becomes

$$\Delta = -\frac{2}{3\pi} \frac{p}{L} \exp[-2\pi\delta L/p]. \tag{29}$$

The dependence of the DM lifetime on the position of ω_D inside the stop band in the limit of thick CLC layers ($|q|L \gg 1$) is shown in Fig. 9, where the results of calculations according to (28) are presented for the frequency range inside the stop band, where the condition $|q|L \gg 1$ holds.

The value of Δ found from (28) and (29) can be regarded as an initial approximation in numerical calculations in the case of an arbitrary CLC layer thickness L . The same result for the DM lifetime τ_D for thick CLC layers in a DM structure ($|q|L \gg 1$) follows from Eq. (22) for the finite lifetime resulting from the electromagnetic wave leakage from the DM structure:

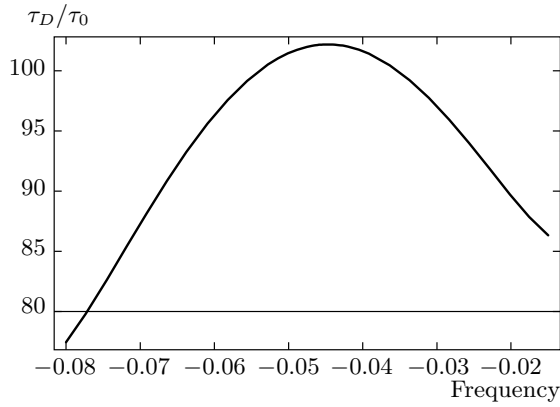


Fig. 9. The DM lifetime (normalized by the time $\tau_0 = 2L\sqrt{\varepsilon_0}/c$ of light flight through the DM structure) dependence on the DM frequency ω_D location inside the stop band calculated for thick CLC layers according to Eq. (28) ($\delta = 0.05$, $N = 40$, and the frequency of the middle point of the stop band corresponds to the abscissa value -0.05)

$$\tau_D = \left(\frac{\delta\kappa^2}{\tau q}\right)^2 \frac{L\sqrt{\varepsilon_0}}{2c} \frac{1}{\delta^2 q L} \times \left\{ \left[\left(\frac{\tau}{2\kappa}\right)^2 + \left(\frac{q}{\kappa}\right)^2 - 1 \right]^2 + \left| \left(\frac{\tau q}{\kappa^2}\right)^2 \right| \right\} \times \exp(2|q|L). \quad (30)$$

For the DM frequency at the middle of the stop band, Eq. (30) gives

$$\tau_D = \frac{3\pi\sqrt{\varepsilon_0}}{\tau c} \frac{L}{p} \exp\left(2\pi\delta\frac{L}{p}\right).$$

Again, as was already mentioned above, the maximum of the DM lifetime τ_D corresponds to the location of the DM frequency just in the middle of the stop band (i. e., at $\kappa = \tau/2$), where $|q|$ reaches a maximum.

11. ABSORBING LIQUID CRYSTAL

We now examine formulas (13) and (14) for absorbing CLC layers. This case, for example, is directly related to the lasing in CLC: at the lasing frequency, the CLC has to be amplifying, whereas at the frequency of the pumping wave, it is absorbing. To take the absorption into account, we let γ be the ratio of the dielectric constant imaginary part to the real part of ε , i. e., $\varepsilon = \varepsilon_0(1 + i\gamma)$. We note that $\gamma \ll 1$ in real situations. A natural consequence of the nonzero absorption ($\gamma > 0$) is a reduction in the transmission and reflection

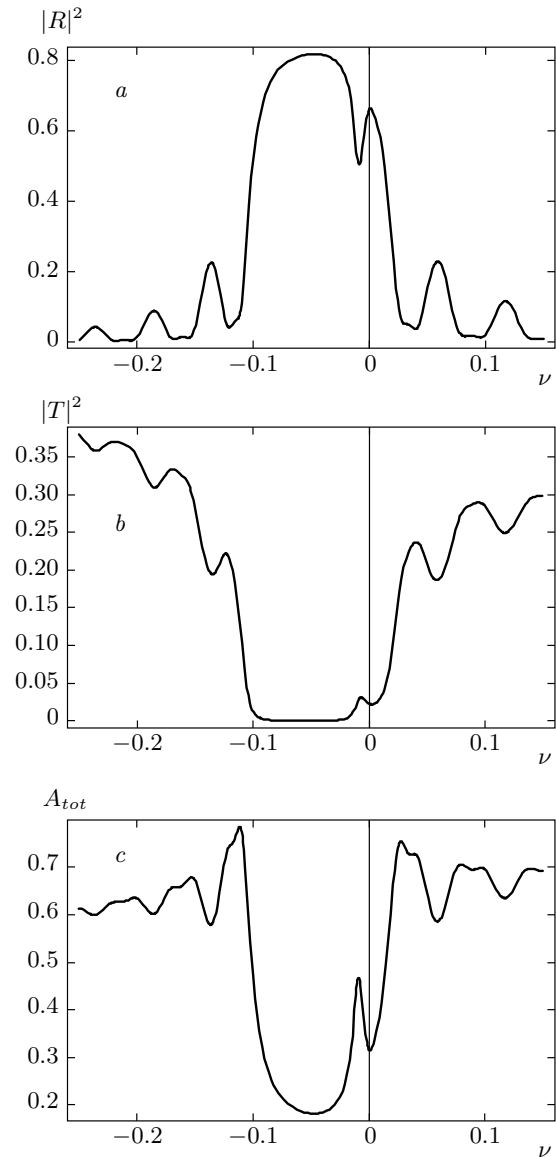


Fig. 10. Reflection (a) and transmission (b) coefficients and the total absorption A_{tot} (c) versus the dimensionless frequency for an absorbing CLC, $\gamma = 0.005$, $d/p = 0.1$, $\delta = 0.05$, and $N = 33$

coefficients. However, there are some interesting peculiarities of the optical properties of the structure under consideration (see Fig. 1). The calculation results presented in Figs. 10–13 reveal these peculiarities. For absorbing structures, $|T(d, L)|^2 + |R(d, L)|^2 < 1$, and the quantity $A_{tot} = 1 - |T(d, L)|^2 - |R(d, L)|^2$ presented in Figs. 10–13 gives the total absorption in the structure. Up to a relatively strong absorption ($\gamma = 0.005$ in Fig. 10), the spectral shapes of the reflection and transmission curves are typical for the DM minima and

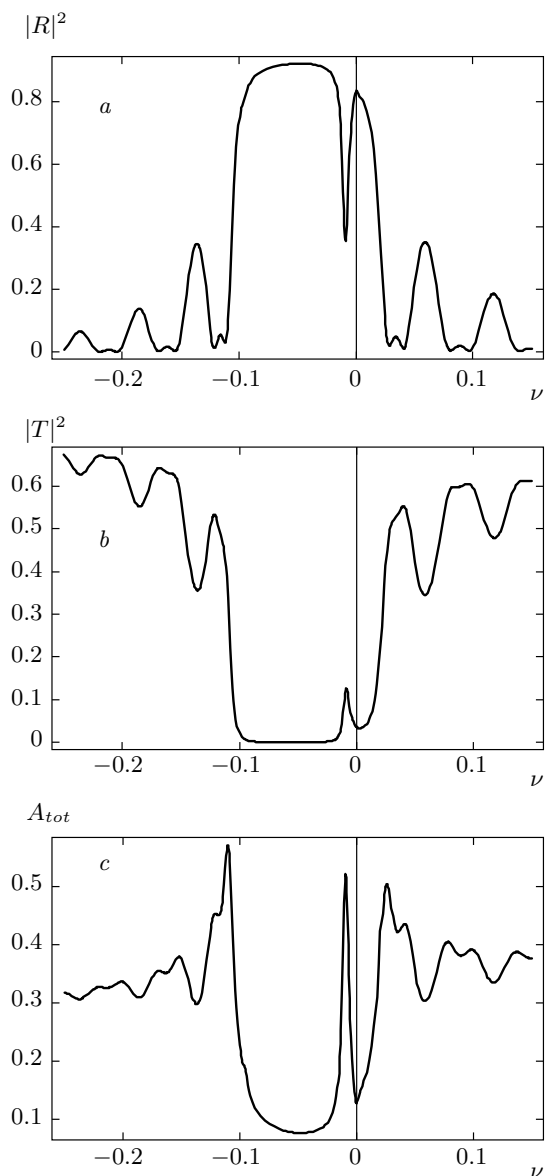


Fig. 11. The same as in Fig. 10 for $\gamma = 0.002$

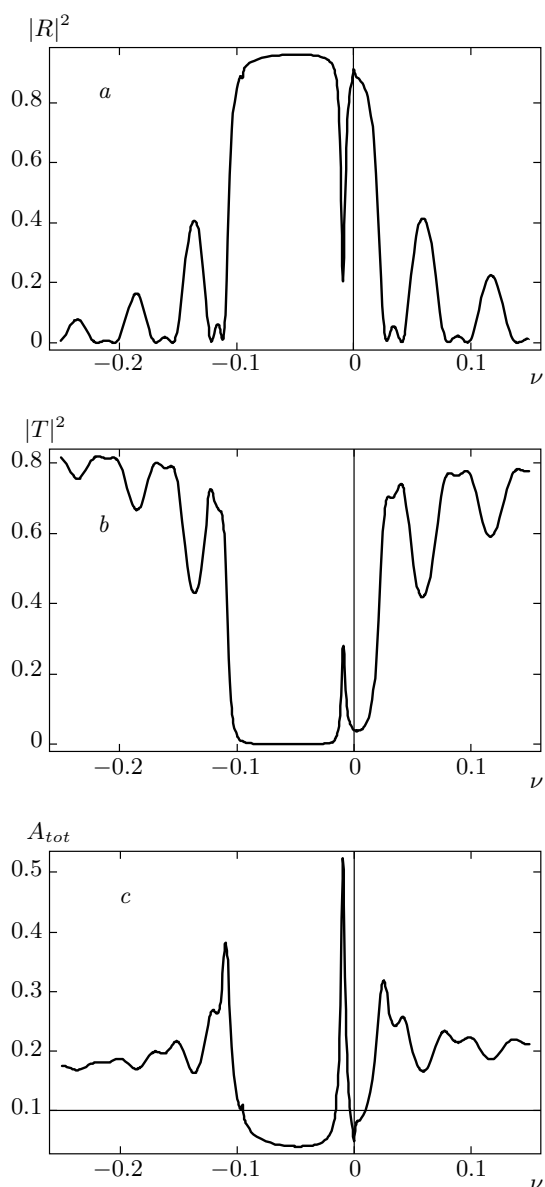


Fig. 12. The same as in Fig. 10 for $\gamma = 0.001$

maxima in the reflection and transmission coefficients, although they deviate from the case of a nonabsorbing CLC (see Figs. 2 and 3). As γ decreases, the spectral shapes of reflection and transmission curves almost approach the corresponding shapes for a nonabsorbing CLC (see Fig. 13a,b corresponding to $\gamma = 0.0003$), but the total absorption at the DM frequency behaves unusually.

As regards the total absorption, it demonstrates a nonconventional frequency dependence. At small γ for some frequencies, the absorption turns out to be much greater than the absorption outside the stop band (see Figs. 10–13). If γ is not too small (Fig. 10c, $\gamma = 0.005$),

the total absorption increase reveals itself at the stop band edges (at the frequencies of the stop band edge modes). This is a manifestation of the so-called anomalously strong absorption effect known for perfect CLC layers at the edge mode frequency [20, 23]. For smaller γ , the total absorption begins to exceed the absorption outside the stop band at the DM frequency ω_D that has the same value as for the stop band edge modes (Fig. 11c, $\gamma = 0.002$). As γ decreases further, the anomalously strong absorption effect becomes more pronounced at the DM frequency than at the edge mode frequencies (Fig. 12c, $\gamma = 0.001$ and Fig. 13c,

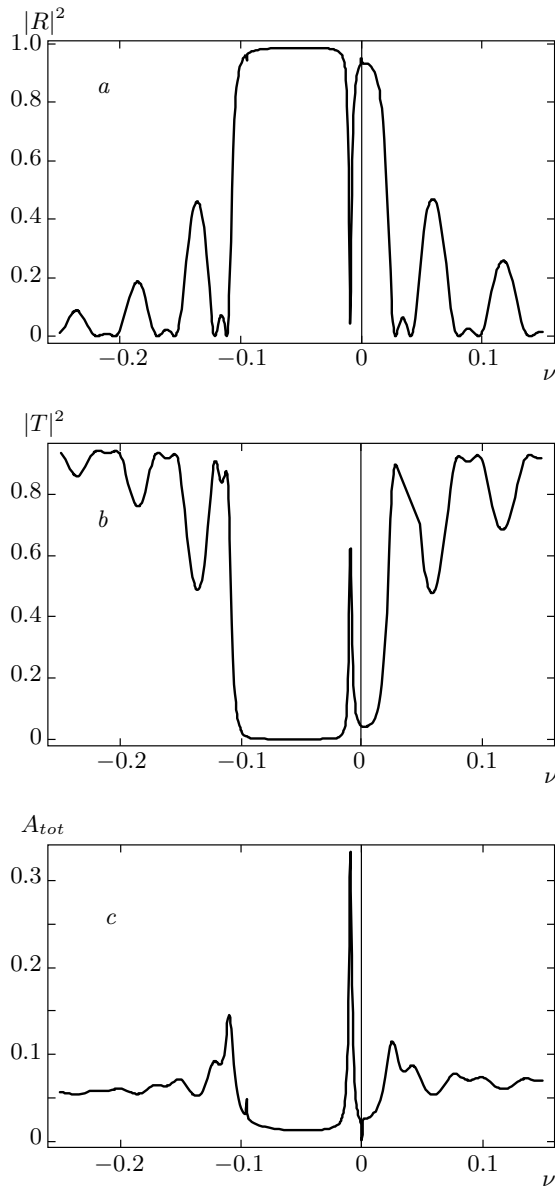


Fig. 13. The same as in Fig. 10 for $\gamma = 0.0003$

$\gamma = 0.0003$). It follows that at the DM frequency ω_D , the effect of anomalously strong absorption similar to the one for the edge mode [23,24] exists and, moreover, the absorption enhancement for the DM at small γ is higher than for the edge mode. It is clear that the anomalously strong absorption effect at the DM frequency is solely due to the localized DM, i.e., to the defect layer in the structure. Its realization assumes some relation between γ and other parameters of the liquid crystal. This relation is determined by the condition

$$\frac{\partial A_{tot}}{\partial \gamma} = 0. \tag{31}$$

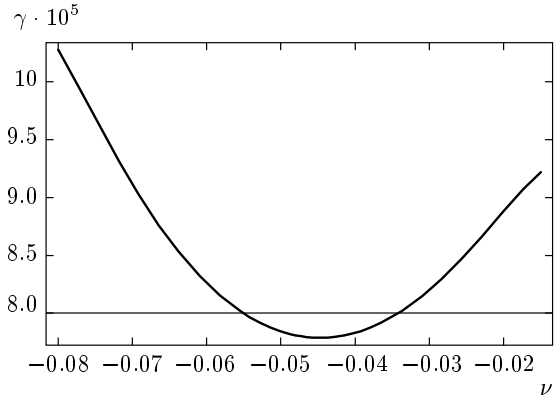


Fig. 14. The gain γ corresponding to a maximum absorption versus the DM frequency location inside stop band is calculated for thick CLC layers according to Eq. (32); $\delta = 0.05$, $N = 40$, and the frequency of the middle point of stop band corresponds to the abscissa value -0.05

In the general case, Eq. (31) can be solved only numerically. But in the case of thick CLC layers ($|q|L \gg 1$), the dependence of γ on L and other parameters ensuring the maximal absorption can be found analytically:

$$\gamma = -\frac{4i\kappa^2 e^{-2|q|L}}{q^2 \tau L} + \left[1 + \frac{1/2 \sqrt{(\tau/\kappa)^2 + \delta^2} - (\tau/2\kappa)^2}{1 - \sqrt{(\tau/\kappa)^2 + \delta^2} + (\tau/2\kappa)^2} \right]^{-1}. \tag{32}$$

The value of γ given by Eq. (32) may be regarded as an initial approximation in numerical calculations in the case of an arbitrary CLC layer thickness L . In Fig. 14, the frequency dependence of γ that corresponds to the maximum absorption for a thick CLC in the limit $|q|L \gg 1$ is presented. Figure 14 shows that the maximum absorption enhancement occurs just in the centre of the stop band.

For the position of ω_D just in the middle of the stop band, expression (32) for γ becomes

$$\gamma = \frac{4}{3\pi} \frac{p}{L} e^{-2\pi\delta L/p}. \tag{33}$$

We note that the anomalously strong absorption effect at the DM frequency and its realization under some relation between γ and other liquid crystal parameters reveal themselves in the calculations of the total absorption at the DM frequency as a function of γ performed in [15] (the absorption reaches a maximum at a small finite value of γ , see Fig. 8 in [15]).

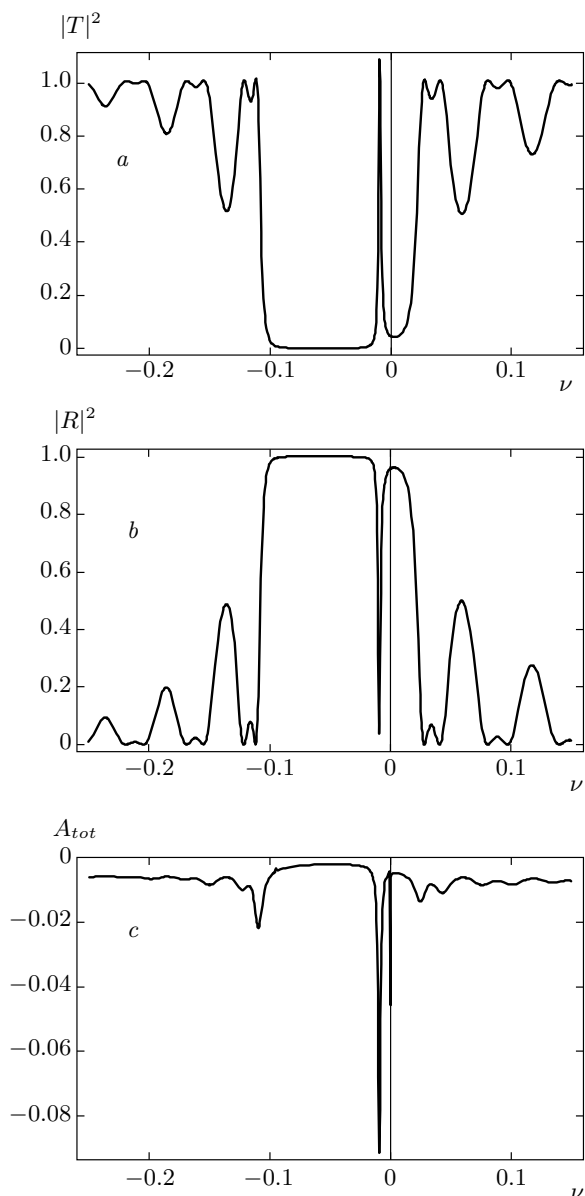


Fig. 15. Transmission (a) and reflection (b) coefficients and the total absorption (c) for an amplifying CLC versus the dimensionless frequency for $\gamma = -0.00005$, $d/p = 0.1$, $\delta = 0.05$, and $N = 33$

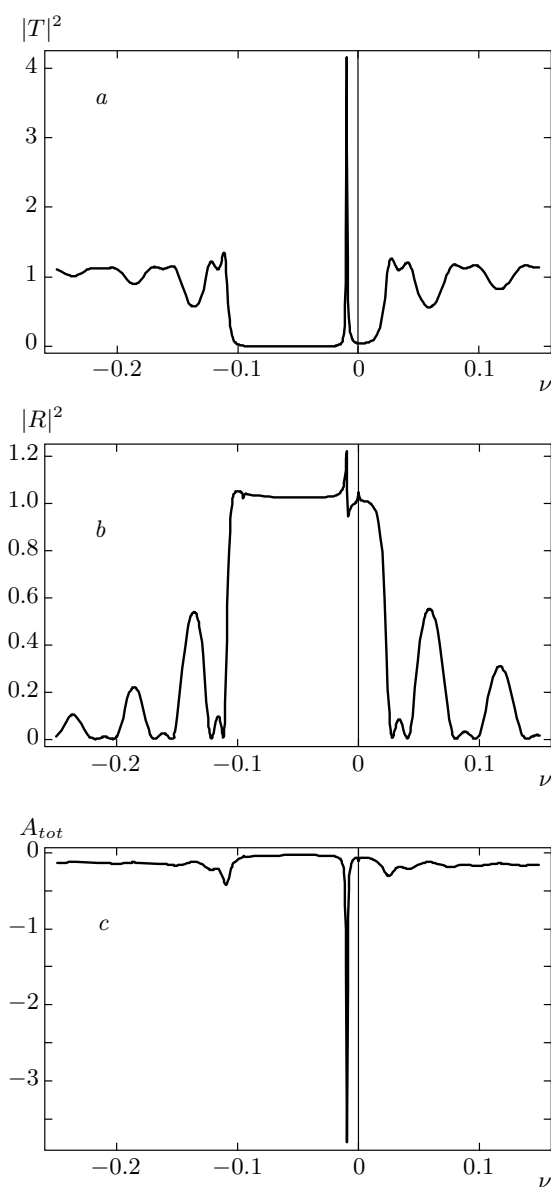


Fig. 16. The same as in Fig. 15 for $\gamma = -0.0006$

12. AMPLIFYING LIQUID CRYSTAL

We examine formulas (13) and (14) for amplifying cholesteric layers. As previously, we assume that the dielectric constant is given by the same formula $\varepsilon = \varepsilon_0(1 + i\gamma)$, but with $\gamma < 0$. The calculation results for the transmission and reflection coefficients at $\gamma < 0$ are presented in Figs. 15–18. For small absolute values of γ , the shape of the transmission and reflection

coefficients is qualitatively the same as for zero amplification ($\gamma = 0$) (Figs. 15a,b). But the absorption is a small negative quantity (which means amplification) at all frequencies with some amplification enhancement at the DM frequency and at the edge mode frequencies (Fig. 15c). As the absolute value of γ increases, the shape of the reflection coefficient $|R(d, L)|^2$ changes at some value of γ (a typical minimum in $|R(d, L)|^2$ is superseded by a small maximum close to 1 and the transmission $|T(d, L)|^2$ exceeds 1 noticeably (Fig. 16)). As the absolute value of γ increases further, the reflec-

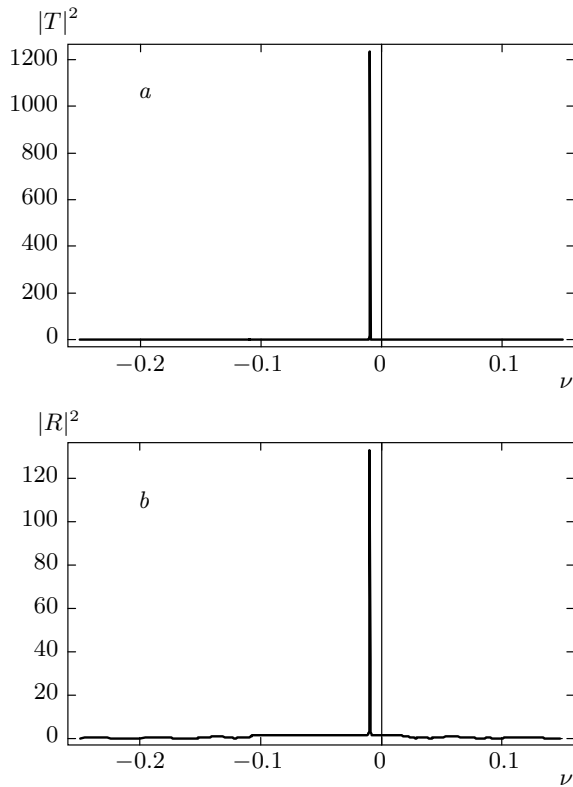


Fig. 17. The same as in Fig. 15 for $\gamma = -0.00117$

tion and transmission coefficients at the DM frequency for the chosen values of the problem parameters exceed 100 (Fig. 17), with no signs of noticeable maxima at other frequencies. The corresponding value of γ may be regarded as being close to the threshold value of the gain γ for the distributed feedback lasing at the DM frequency. With the continuing increase in the absolute value of γ , we find that diverging maxima of $|R(d, L)|^2$ at the edge mode frequencies appear (without traces of a maximum at the DM frequency) for the gain five time greater than the threshold gain for the DM (Fig. 18). At even greater absolute values of γ , we find that new edge mode frequencies, more distant from the stop band edge [22, 24], appear. The observed result shows that the DM lasing threshold gain is lower than the corresponding threshold for the stop band edge modes. Another conclusion following from this study is the revealed existence of some interconnection between the liquid crystal parameters at the lasing threshold, which for thick CLC layers was found analytically for the DM (see Eq. (34)) and for edge modes (see [22, 24]). In fact, a continuous increase in the gain results in the appearance of lasing at new modes, with the disappearance of lasing at the previous modes cor-

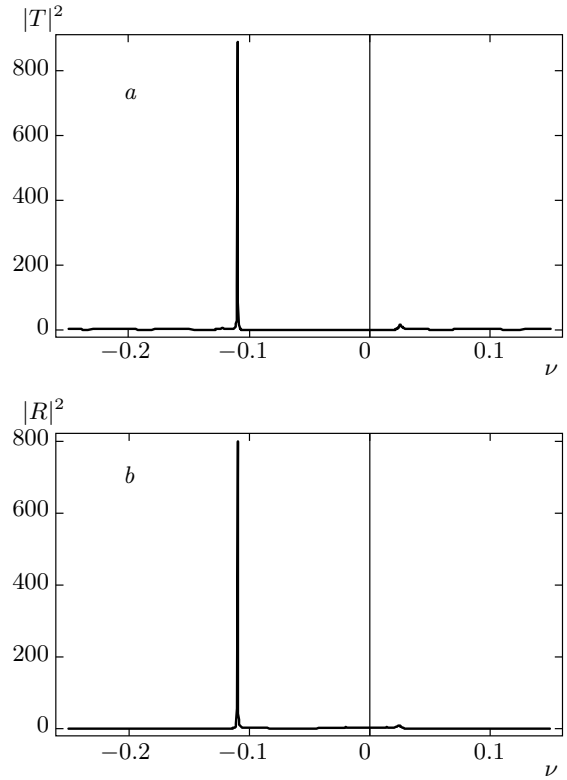


Fig. 18. The same as in Fig. 15 for $\gamma = -0.0045$

responding to lower thresholds (this was observed experimentally in [3]).

To find the interconnection between the liquid crystal parameters at the lasing threshold mentioned above, we have to solve the DM dispersion equation following from Eq. (18) under the assumption that the CLC layers are amplifying ($\gamma < 0$). In the general case, this should be done numerically. But in the case of thick CLC layers ($|q|L \gg 1$), the dependence of the threshold γ on L and other parameters can be found analytically. For example, if the DM frequency ω_D is located at the stop band center, the corresponding relation for the threshold gain is given by

$$\gamma = -\frac{4}{3\pi} \frac{p}{L} e^{-2\pi\delta L/p}. \quad (34)$$

The exponentially small value of $|\gamma|$ following from Eq. (34) for thick CLC layers confirms the above statement about lower lasing threshold for the DM compared to the edge mode. In fact, the lasing threshold for the edge mode for thick CLC layers does not decrease exponentially with L , but is inversely proportional to only the third power of L .

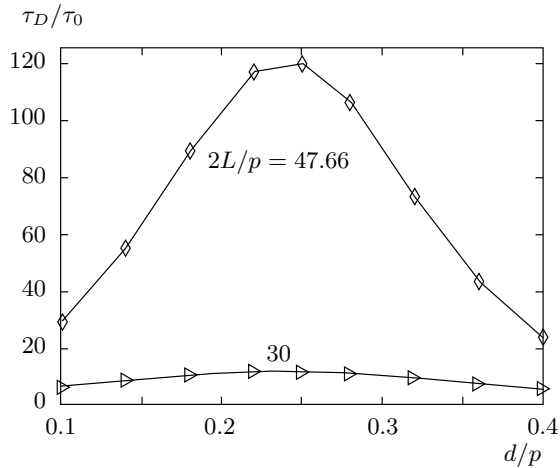


Fig. 19. The DM lifetime (normalized by the time $\tau_0 = 2L\sqrt{\varepsilon_0}/c$ of light flight through the DM structure) dependence on the defect layer thickness found numerically for two values of the CLC layers thicknesses L ($\delta = 0.05$)

13. CALCULATION RESULTS

The above plots obtained analytically in the limit cases may be compared with numerical calculations performed for the problem parameters corresponding to their typical values in experiment. Figure 19 presents the calculated values of the DM lifetime as a function of the defect layer thickness d/p at a fixed CLC layer thickness L . Figure 20a presents the calculated values of the lasing threshold $|\gamma|$ as a function of the defect layer thickness d/p at a fixed CLC layer thickness L . Figure 21b presents the calculated values of the lasing threshold $|\gamma|$ as a function of the CLC layer thickness L . In the applicability range of the analytic approach, the analytic and calculated values are in good agreement. In particular, Fig. 21b reveals that the lasing threshold $|\gamma|$ exponentially decreases with an increase in the CLC layer thickness L for thick layers in the middle of the stop band ($d/p = 0.25$), but at the same thicknesses L close to the stop band edge ($d/p = 0.1$), where the limit of thick layers is inapplicable, there are deviations from the exponential decrease.

14. CONCLUSION

Our analytic description of the DMs neglecting the polarization mixing at the CLC boundaries in the structure under consideration allows revealing a clear physical picture of these modes, which is applicable to the DMs in general. For example, a lower lasing threshold

and stronger absorption (under the conditions of the anomalously strong absorption effect) at the DM frequency compared to the edge mode frequencies are the features of any periodic media. We note that the experimental studies of lasing threshold [3] agree with the corresponding theoretical result obtained above. Moreover, the experiment in [3] also confirms the existence of some interconnection between the gain and other liquid crystal parameters at the threshold pumping energy for lasing at the DM (as well at the stop band edge mode) frequency. Specifically, this was demonstrated by the observations that an increase in the pumping energy above the threshold value results in a decrease in the lasing intensity (see Fig. 5 in [3]).

For a special choice of the parameters in the experiment, the obtained formulas may be directly applied to the experiment. Nevertheless, it should be kept in mind that direct comparison of the theory and experiment requires some conditions to be met. For example, the defect layer thickness variations should be less than the light wavelength. For comparison with a real experiment, the dielectric susceptibility frequency dispersion must also be taken into account. In the general case, however, a mutual transformation at the boundaries of the two circular polarizations of opposite sense must also be taken into account. For example, the circular polarization sense observed in experiment [3] for the wave emitted from the defect structure above the lasing threshold may be opposite to the polarization sense responsible for the DM existence. An evident explanation of the “lasing” at the opposite (nondiffracting) circular polarization is as follows. Due to the polarization conversion of the generated wave into a wave of the opposite circular polarization, the converted wave of a nondiffracting polarization freely escapes from the structure. This polarization conversion phenomenon also contributes to the frequency width of the DM. Therefore, polarization mixing must also be taken into account in calculations of the DM lifetime (frequency width). In the general case, the DM field leakage from the structure is also determined by the finite CLC layer thickness, and hence by the leakage due to the polarization conversion. Only for sufficiently thin CLC layers or in the case of the DM frequency being very close to the stop band frequency edges, the main contribution to the frequency width of the DM is determined by the thickness effect and the model developed above may be directly applied for describing experimental data.

Our model allows obtaining results that may simulate polarization conversion and may be quantitatively applicable for the experiment description. Because the polarization conversion at the CLC surfaces is of the

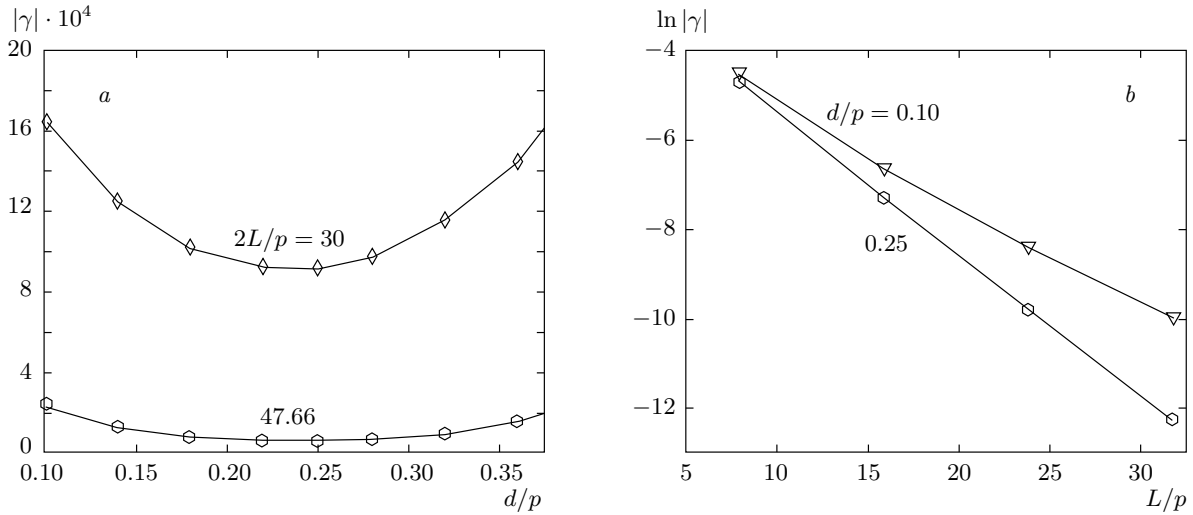


Fig. 20. Lasing threshold at the DM frequency versus the defect layer thickness (a) and the CLC layers thickness (b) found numerically for two values of the CLC layer thickness L ($\delta = 0.05$)

order of the dielectric anisotropy δ (in the absence of reflection at a dielectric boundary) [20, 21], the analysis of the problem in the framework of our model and its results would correspond to a real situation for very thick CLC layers if the CLC layer thickness L is assumed to be less than the actual CLC layer thickness, and would correspond to the transmission coefficient of the CLC layer inside the stop band being approximately equal to the CLC anisotropy δ . And, more generally, for a real structure with a layer thickness L , the structure with the CLC layer thickness less than L has to be considered in our approach for simulation of the polarization conversion. We note that the applied analytic approach helped reveal the anomalously strong absorption effect at the DM frequency. The corresponding “observation” would be much more difficult to do in a purely numerical approach.

The defect type considered above is a homogenous layer. The developed approach is also applicable to a defect of the “phase jump” type [2, 3, 15, 16], and the corresponding results are practically the same as above. Namely, the equation related to the case of a “phase jump” defect is obtained from the equations presented above by substituting the quantity $2\Delta\varphi$ instead of $2\kappa d$ in the factor $\exp(2i\kappa d)$, where $\Delta\varphi$ is the spiral phase jump at the defect plane. Based on the present results, we may point out in advance one difference between the two types of defects. Namely, for a phase jump defect, in contrast to the considered homogenous layer defect, only one DM frequency inside the stop band frequency range is possible because the value of the phase jump

is limited by the condition $|\Delta\varphi| \leq 2\pi$. In particular, the DM frequency for a phase jump defect is located at the stop band center at $|\Delta\varphi| = \pi/2$.

We also note that the localized DMs (as well as the edge modes) reveal themselves in an enhancement of some inelastic and nonlinear optical processes in photonic liquid crystals. For example, we mention the experimentally observed effects of the enhancement of nonlinear optical second harmonic generation [25] and lowering of the lasing threshold [26] in photonic liquid crystals, along with the theoretically predicted enhancement of Cherenkov radiation (Sec. 4 in [20] and Ch. 5 in [21]).

To conclude, we state that the results obtained here for the DMs (see also [27]) and in Refs. [22, 24] for the edge modes clarify the physics of these modes and entirely agree with the previous numerical results [28]. Our results are qualitatively applicable to the corresponding localized electromagnetic modes in any periodic media and may be regarded as a useful guide in the studies of localized modes in general.

The work is supported by the RFBR (grants Nos. 09-02-90417-Ukr_f_a and 10-02-92103-Jp_a).

REFERENCES

1. Y.-C. Yang, C.-S. Kee, J.-E. Kim et al., Phys. Rev. E **60**, 6852 (1999).
2. V. I. Kopp and A. Z. Genack, Phys. Rev. Lett. **89**, 033901 (2003).

3. J. Schmidtke, W. Stille, and H. Finkelmann, *Phys. Rev. Lett.* **90**, 083902 (2003).
4. P. V. Shibaev, V. I. Kopp, and A. Z. Genack, *J. Phys. Chem. B* **107**, 6961 (2003).
5. E. Yablonovitch, T. J. Gmitter, R. D. Meade et al., *Phys. Rev. Lett.* **67**, 3380 (1991).
6. I. J. Hodgkinson, Q. H. Wu, K. E. Torn et al., *Opt. Comm.* **184**, 57 (2003).
7. H. Hoshi, K. Ishikawa, and H. Takezoe, *Phys. Rev. E* **68**, 020701(R) (2003).
8. A. V. Shabanov, S. Ya. Vetrov, and A. Yu. Karneev, *Pis'ma v Zh. Exp. i Teor. Fiziki* **80**, 206 (2004).
9. I. J. Hodgkinson, Q. H. Wu, K. E. Thorn, A. Lakhtakia, and M. W. McCall, *Opt. Comm.* **184**, 57 (2000).
10. F. Wang and A. Lakhtakia, *Opt. Express* **13**, 7319 (2005).
11. M. H. Song, N. Y. Ha, K. Amemiya et al., *Adv. Mater.* **18**, 193 (2006).
12. H. Yoshida, C. H. Lee, A. Fuji, and M. Ozaki, *Appl. Phys. Lett.* **89**, 231913 (2006).
13. H. Yoshida, R. Ozaki, K. Yoshino, and M. Ozaki, *Thin Solid Films* **509**, 197 (2006).
14. A. H. Gevorgyan and M. Z. Haratyunyan, *Phys. Rev. E* **76**, 031701 (2007).
15. M. Becchi, S. Ponti, J. A. Reyes, and C. Oldano, *Phys. Rev. B* **70**, 033103 (2004).
16. J. Schmidtke and W. Stille, *Eur. Phys. J.* **90**, 353 (2003).
17. H. de Vries, *Acta Crystallogr.* **4**, 219 (1951).
18. E. I. Kats, *Zh. Eksp. Teor. Fiz.* **59**, 1854 (1970).
19. P. G. de Gennes, and J. Prost, *The Physics of Liquid Crystals*, Clarendon Press, Oxford (1993).
20. V. A. Belyakov and V. E. Dmitrienko, in *Sov. Sci. Reviews A Phys., Sec. — Vol. 13*, ed. by I. M. Khalatnikov, Harwood Press, London (1989), p. 54.
21. V. A. Belyakov, *Diffraction Optics of Complex Structured Periodic Media*, Springer-Verlag, New York (1992), Ch. 4.
22. V. A. Belyakov and S. V. Semenov, *Zh. Eksp. Teor. Fiz.* **136**, 797 (2009); *Mol. Cryst. Liq. Cryst.* **507**, 209 (2009).
23. V. A. Belyakov, A. A. Gevorgian, O. S. Eritsian, and N. V. Shipov, *Zh. Tekhn. Fiz.* **57**, 1418 (1987); *Kristallografiya* **33**, 574 (1988).
24. V. A. Belyakov, *Mol. Cryst. Liq. Cryst.* **453**, 43 (2006); *Ferroelectrics* **344**, 163 (2006).
25. K. Shin, H. Hoshi, D. Chang et al., *Opt. Lett.* **27**, 128 (2002).
26. Y. Matsuhisa, Y. Huang, Y. Zhou et al., *Appl. Phys. Lett.* **90**, 091114 (2007).
27. V. A. Belyakov, *Mol. Cryst. Liq. Cryst.* **494**, 127 (2008).
28. V. I. Kopp, Z.-Q. Zhang, and A. Z. Genack, *Progr. Quant. Electron.* **27**, 369 (2003).